Ultrafine Grained Materials IV. *Edited by Y.T. Zhu, T.G. Langdon, Z. Horita, M.J. Zehetbauer, S.L. Semiatin, and T.C. Lowe.* **TMS (The Minerals, Metals & Materials Society), 2006**

TRANSMISSION ELECTRON MICROSCOPY STUDY OF THE STRAIN INDUCED LOW AND HIGH ANGLE BOUNDARY DEVELOPMENT IN EQUAL-CHANNEL ANGULAR-PRESSED COMMERCIALLY PURE ALUMINUM

M. Cabibbo[1,*], E. Evangelista[1], M.E. Kassner[2], M.A. Meyers[3]

[1]CNR-(INFM)/Dept. of Mechanics, Polytechnic University of Marche
Via Brecce Bianche, 60131-Ancona, Italy
[2]Dept. of Aerospace and Mechanical Engineering, University of Southern California
Los Angeles, CA, 90089-1453, USA
[3]Mechanical and Aerospace Engineering Department, University of California, San Diego
La Jolla, CA, 92093-0411, USA

Abstract

Cell and high-angle grain boundary evolution under equal channel angular pressing (ECAP) was investigated in commercially pure aluminum using transmission electron microscopy. Transmission electron microscopy techniques were extensively used to characterize very low-angle (i.e. less than 1.5 – 2°) boundaries, which are difficult, if not impossible, to detect by field-emission gun scanning electron microscopy with electron back-scattered diffraction. Boundary misorientation was measured by Kikuchi pattern and performed across about 120 boundaries at each pass (strain level). Early, very low-angle boundaries were mostly characterized using Moiré fringes, which yielded a more precise value of lattice angular misorientation across each boundary. Following route Bc to a true strain of 8, the microstructure mainly consisted of nano-scale grains and high-angle boundaries (misorientations higher than 15°) accounted for ~70% of all boundaries. The microstructural evolution was compared with that induced by cold-rolling (CR) to equivalent strains. The substructure development generally exhibits the same trends, as a function of strain, for both ECAP and CR and have very similar grain refining potentials.

Keywords: TEM, geometric necessary boundaries, incidental dislocation boundaries, ECAP, nanostructure

Introduction

Different techniques for producing ultrafine-grained (UFG) materials for structural applications have been introduced, especially over the last decade [1]. The advantages of fabricating materials with sub-micron size grain microstructures as structural components lie in their improved mechanical properties such strength, hardness, ductility, fatigue resistance and low-temperature superplasticity [1-10]. Equal channel angular pressing (ECAP) is one promising technique that uses severe plastic deformation (SPD) to induce a refined microstructure. ECAP has the important advantage of maintaining billet shape. This method was introduced and developed by Segal et al. [2]. A typical ECAP die consists of two intersecting channels of identical cross-section [1-3]. A billet of material is introduced in the vertical channel and forced by a plunger into the horizontal channel [3]. The shear strain per pass through the die is determined by the channel angle and the intersecting curvature

* Corresponding author. m.cabibbo@univpm.it

[6,11,12]. Many processing parameters affect the processed microstructure [12]: die angle (determining the strain introduced into the material), the number of passes (accumulation of strain), deformation route (critical parameter for texture and microstructure evolution with strain), and the extrusion speed, temperature, friction. Langdon and co-workers [9-11] found that a die angle of 90° is the most efficient, while the extrusion speed and specimen - die channel friction being of only minor influence on the refining process. As temperature decreases, the load needed to press the billet reduces. A number of theories have been proposed to explain the effect of processing routes on the microstructure.

Furukawa and co-workers [11] proposed that route Bc (90° rotation of the billet after each pass) is most favorable for producing a microstructure consisting of essentially uniform and relatively equiaxed grains separated by high-angle boundaries (HABs). This was suggested to be due to the development of a shear on mutually crossing planes, and a regular restoration of equiaxed structure during consecutive pressing. Sun et al. [12,13] studied the different routes as a function of different microstructure parameters and found that, in terms of formation of HABs, A>Bc>C, in terms of reducing grain size, Bc>A>C, and in terms of generating equiaxed grains, Bc>C>A. Systematic studies on cell and grain evolution have been performed only in recent years [4,14-19,23,24]. Several investigations [12,13,20-27,29-33] have shown that, during deformation [23,24], grains in polycrystals subdivide into many small crystallites. Studies on metals established that grains break-up into domains of different slip systems, called cell blocks during deformation [22,27]. Ashby [31] first introduced the concept of geometrically necessary dislocations forming at the interface of the cell blocks in order to maintain compatibility. These are generally referred to as geometrically necessary boundaries (GNBs). Boundaries are also formed by statistically random trapping of dislocations into an array of generally low-angle boundaries, often referred to as incidental dislocation boundaries (IDBs). These are generally interconnecting boundaries that subdivide cell blocks into individual cells [20,22,27-32]. One of the major distinction between the two types of boundary lies in their rather different misorientation scale and the misorientation evolution with strain. The different misorientation ranges between GNBs and IDBs has a physical basis in the sense that GNBs are formed to accommodate lattice rotations during deformation that results in the formation of cell blocks with different slip systems. The boundary spacing and misorientation angle distribution of GNBs and IDBs evolve differently with strain. In particular, they exhibit different morphologies at small to medium strains, but similar morphology at higher strains, in non-ECAP studies [32-37]. Generally, misorientation axes for IDBs are randomly distributed, whereas GNB orientation distribution clusters on preferred axes. Some GNBs show a pattern of rotation around the transverse direction in a plane containing the extruded (pressing) and transverse directions in ECAP [24,34].

This study aimed at gaining insights into the IDB / GNB evolution from a low- to medium-angle boundary character towards high-angle boundary (HAB) formation in severely deformed AA1200 aluminum. The microstructure evolution is described on the basis of formation and evolution of IDBs and GNBs, consistent with the recent work of Sun et al. [23,24]. The microstructural evolution in ECAP is also compared with the structure evolution generated by cold rolling (CR). The two parameters chosen for the comparison are the spacing between the GNBs and IDBs, and the angle of misorientation across these boundaries. The misorientation angles were measured using Kikuchi pattern analyses by TEM.

Experimental Procedure

The chemical composition of the AA1200 used in this study is: 0.7% Si, 0.3% Fe, 0.1% Zn, 0.05% (Cu+Mn). The material was produced, as extruded and homogenized rods, by Hydro Aluminium with a diameter of 10 mm. The rods were cut into 10 cm lengths. The initial mean grain size was 80 μm. ECA pressing was performed at room temperature using

a solid die fabricated from a block of SK3 tool steel (Fe-1.1%C) with two cylindrical channels intersecting at an angle $\Phi = 90°$ and a curvature $\Psi = 20°$ [38]. The pressing speed of the plunger was ~8 mm·s^{-1} and pressures were in the range of 20 to 70 kN. Samples and channels were coated with a spray lubricant containing MoS_2. Deformation route Bc was used with 90° billet rotation subsequent to every pass. ECAP was performed using 8 passes. The Bc route choice was based on the capability of producing the minimum grain size (i.e. the maximum efficiency in refining the microstructure) and inducing a high fraction of HABs among the possible ECAP routes [9,10,12], as discussed earlier. Specimen surfaces were anodized along the ED-TD plane (i.e. the extrusion-transverse direction plane, which corresponds to the Y-plane in the Langdon notation [9-12]) for optical microscopy (OM), using a solution of 5% HBF_4 in methanol at a voltage of 20 V and a current of 30 mA at room temperature. TEM samples were sectioned along the ED-TD plane. Thin foils were prepared by mechanically grinding 1-mm thick slices to a thickness of 70-90 μm, followed by chemical polishing (1/3 HNO_3 in methanol) in order to minimize the grinding damage. Foils were subsequently thinned with a double-jet electro-polisher using a solution of 20% $HClNO_4$ and 80% methyl alcohol at -15°C and 24 V. Thin discs were examined in a Philips CM200 TEM operating at 200 kV and equipped with a double-tilt stage. Crystallographic orientations were determined and measured by using Kikuchi pattern across the boundaries consistent with the method of Liu [37]. Microstructure characterization was performed on 3 discs from each deformation condition and 5 different areas on each disc, corresponding to 250-280 boundaries from which the misorientation was measured by either Kikuchi pattern or Moiré fringes. Three independent Kikuchi patterns were utilized in measuring the misorientation across boundaries (typically either IDBs and GNBs). Misorientation measurement via Moiré fringes was preferentially performed because of the ease and quickness of the evaluation, although only a small fraction of boundaries (less than ~5%) were evaluated by this procedure.

Results and Discussion

Figure 1 is a polarized optical micrograph (POM) showing the initial microstructure. As will be discussed later, the 7th and 8th pass eventually reduces the GNB lateral spacing to a mean value of 320 nm, the high-angle boundary fraction rose to ~72% of the total amount of boundaries (original grains, GNBs and IDBs).

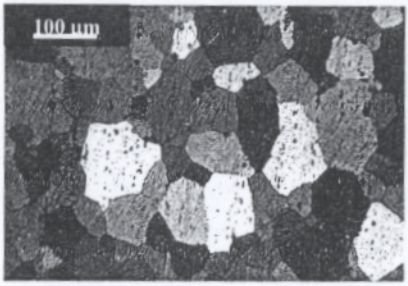

Figure 1. POM image of the un-deformed material.

As the strain increases, the fraction of boundaries that are low-angle boundaries (LABs) decreases steadily. Figure 2 (a) to (d) shows some representative micrographs illustrating the boundary spacing evolution with strain of either IDBs and GNBs. Boundary misorientation angles are also reported.

Figure 3 is a plot of the high-angle boundary fraction as a function of the strain. The high angle ($\Theta > 15°$) fraction reached a value of 72% after the maximum strain of 8, and saturation may have reached. Figure 3 also reports the sub-structure evolution which has been also compared to the one occurring for the same alloy but cold-rolled (data after Hansen (1969) and Shun (1974) reported by Nes in [28]). One sub-structure parameter, that is a microstructure refinement parameter, has been defined as [28]:

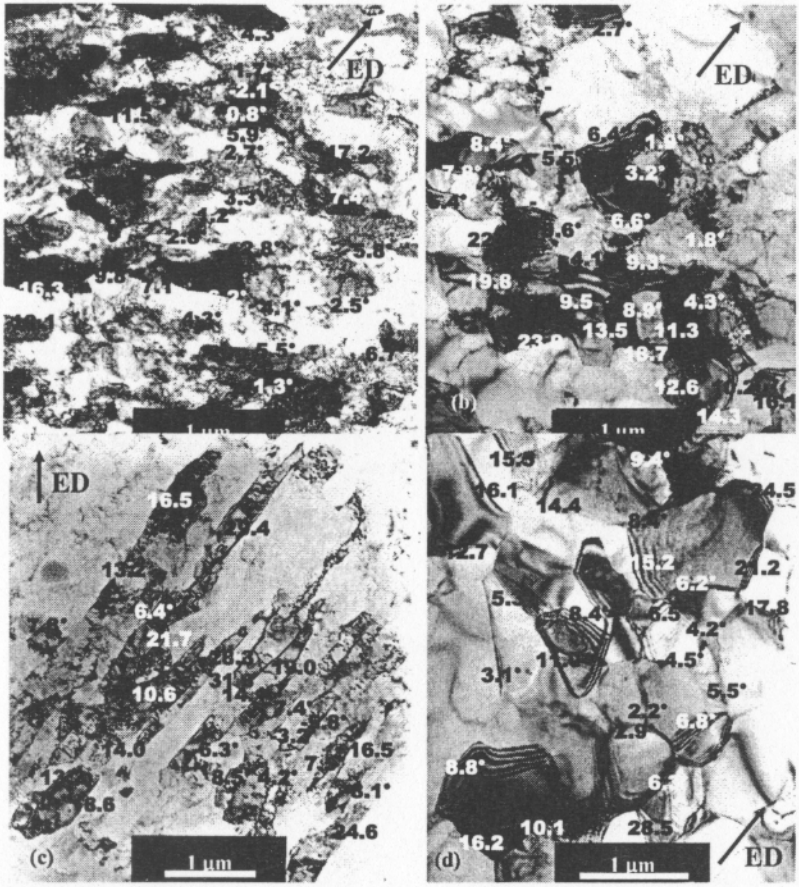

Figure 2. TEM-BF images after 1 (a), 4 (b), 5 (c), 8 passes (d). Some of the boundary misorientation values are also reported. The extruded direction (ED) (i.e., ECA-pressing direction) is indicated.

$$\Delta = 1/(1/\lambda + 1/d) \quad (1)$$

where d and λ are usually defined as the grain and cell size, respectively, but here, are defined as the mean GNB spacing, although some original grain boundaries may be included, and IDB size, respectively (see [28]). The evolution in the common range of strain

for both ECAP and cold-rolling practically overlap. This suggests a similar microstructure refinement mechanism. The refinement decreases asymptotically to a limit of about 0.6 - 0.7 μm.

Figure 4 shows the plot of GNBs (mainly constituted by block walls and some original elongated grain boundaries) ($\Theta > 15°$) and IDBs (low-angle boundaries, which are essentially cell walls) misorientation as a function of the strain. IDBs have an average constant misorientation value $\Theta \cong 3°$ with increasing strain, while GNBs revealed a constant

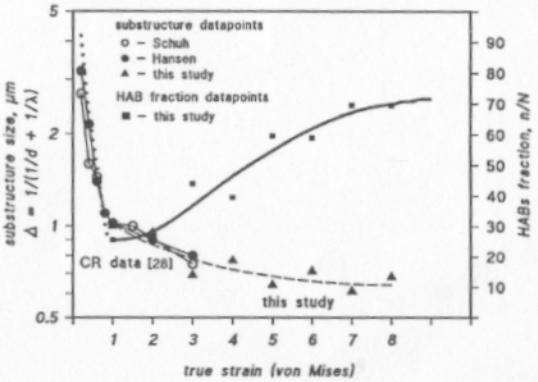

Figure 3. Substructure spacing evolution [$\Delta = (1/\lambda + 1/d)$], and HAB (generally GNB), fraction as a function of the true strain (also the number of ECAP passes). Substructure spacing data were also compared with those reported by E. Nes [28] in relation to some Al-alloys subjected to cold rolling. In the substructure relationship, d represents the mean grain size, and λ the cell size. Open and solid circle data points refer to commercially pure Al data reported in [29], while solid up-triangle data points refer to AA 1200 ECA-pressed material of this study.

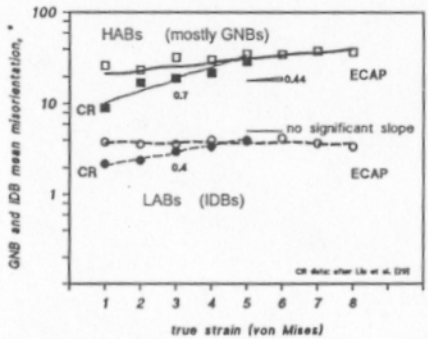

Figure 4. High angle boundary (generally GNB) and low angle boundary (IDB) misorientation as a function of true strain. Solid data points cold-rolled (CR) [18], open points to ECAP (present study). Circle points are IDBs, squared, GNBs.

positive slope of 0.44. Hughes and Hansen [17,18,23] report slopes of 0.7 and 0.4 for GNBs and IDBs, respectively, in cold-rolled aluminum. The ECAP microstructure may be more equiaxed than that of cold rolling because of the reversed shearing in ECAP. Figures 3 and 4

illustrate a similar deformation cell and grain size formation and evolution but slightly different boundary misorientation evolution.

Figure 5 (a) and (b) are a plot of HAB (defined as boundaries with a misorientation higher than 15°) and LAB (boundary misorientation up to 15°) mean spacing and misorientation distributions as a function of strain. As the strain increases, the distribution of HAB spacing moves toward lower values with a significant narrowing. Thus, the peak maximum moves from about 3.5 μm at the 1st pass, to<1.0 μm after the 8th pass. The LAB

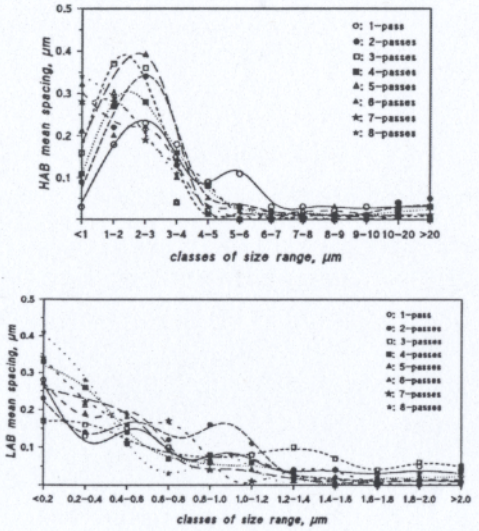

(a)

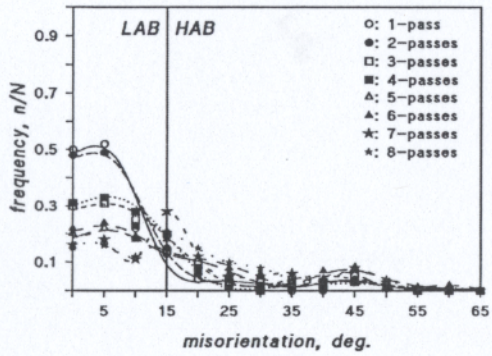

(b)

Figure 5: Plot of the average high-angle boundary (HAB) and low-angle boundary (LAB) spacing as a function of strain (a), HAB and LAB misorientation distribution with strain (b). The average values (n/N) are made from a boundary population, N, of 250-280 boundaries per deformation condition.

distribution appears to spread to a wide range of sizes range, and again there is a lowering mean spacing from the 1st to the 8th pass. The misorientation distribution of all (LABs and HABs) boundaries is shown in Fig. 5 (b). By a strain of 8, nearly 70% of all boundaries are high angle (Θ>15°).

The plastically deformed microstructure is dominated by almost parallel shear bands (essentially GNBs) forming angles of roughly 45° respect to the pressing direction. The deformed microstructure consisted of highly elongated grains and GNBs fragmented by transverse LABs (IDBs), which tend to become equiaxed after each even number of passes. Thus, the mechanism of microstructure refinement and HAB generation with strain is due to a grain subdivision by the introduction of mutually crossing GNBs. This process has been described by Hughes and Hansen [29] for CR and by Sun et al. [21,22] for ECAP. Sun in [23], using the same strain path (i.e., route Bc), also found that the grain subdivision is also strongly influenced by the original grain orientations. CR results in a continuous aspect ratio increment in CR until grain boundary starts pinching. This microstructure evolutional difference with ECAPs accounts for a more homogeneous microstructure refining in ECAP compared to CR.

Conclusions

The low- and high-angle cell and grain boundary evolution induced by equal channel angular pressing in a commercially pure 1200 aluminum alloy was investigated. Transmission electron microscopy techniques were extensively used to characterize very low-angle (i.e. less than 1.5 – 2°) boundaries, which are difficult, if not impossible, to detect by field-emission gun scanning electron microscopy with electron back-scattered diffraction. Boundary misorientation was measured by Kikuchi pattern and performed across about 120 boundaries at each pass (strain level). Early, very low-angle boundaries were mostly characterized using Moiré fringes, which yielded a more precise value of lattice angular misorientation across each boundary.

Following route Bc to a true strain of 8, the microstructure mainly consisted of nano-scale grains and high-angle boundaries (misorientation higher than 15°) accounted for ~70% of all boundaries. The microstructural evolution was compared with the one induced by cold-rolling (CR) to equivalent strains. The substructure parameter (defined as the sum of the reciprocal of cell and grain spacing: $\Delta = 1/\delta + 1/d$) exhibits the same trend, as a function of strain, for either ECAP and CR commercially pure aluminum. However, misorientation of high-angle and low-angle boundaries increased somewhat less with strain in ECAP material. ECAP and CR have very similar grain refining potentials, although the grain equiaxiality is retained in ECAP.

Acknowledgments

Supported by the NSF-European collaboration grant DMR – 041222, and research grant from the INFM PAIS-UFIGRAL project are gratefully acknowledged. The authors wish to thank Dr. V. Latini for her help during ECA pressing. Material supply and specimen machining by Hydro Aluminium, Norway, is gratefully acknowledged.

References

[1] V.M. Segal, V.I. Reznikov, A.E. Drobyshevskiy, V.I. Kopylov, Russian Metallurgy, 1981, 1, 99.

[2] Y.T. Zhu, T.C. Lowe, Mater. Sci. Eng., A291, 2000, 46.

[3] V.M. Segal, Mater. Sci. Eng., A197, 1995, 157.

[4] S.C. Baik, Y. Estrin, H.S. Kim, R.J. Hellmig, Mater. Sci. Eng., A351, 2003, 86.

[5] P.B. Berbon, N.K. Tsenev, R.Z. Valiev, M. Furukawa, Z. Horita, M. Nemoto, T.G. Langdon, Metall. Mater. Trans., A29, 1998, 2237.

[6] Y. Iwahashi, Z. Horita, M. Nemoto, T.G. Langdon, Acta Mater., 46, 1998, 3317.
[7] P.B. Prangnell, J.R. Bowen. Ultrafine Grained Materials-II, Ed. Y.T. Zhu, T.G. Langdon, R.S. Mishra, S.L. Semiatin, M.J. Saran, T.C. Lowe, TMS (The Minerals, Metals & Materials Society) , 2002, 89.
[8] A. Gholina, P.B. Prangnell, M.V. Markushev, Acta Mater., 48, 2000, 1115.
[9] J.Y. Chang, J.S. Yoon, G.H. Kim, Scripta Mater., 45, 2001, 347.
[10] Z. Horita, T. Fucinami, M. Nemoto, T.G. Langdon, Metall. Mater. Trans., A31, 2000, 691.
[11] Y. Iwahashi, M. Furakawa, Z. Horita, M. Nemoto, T.G. Langdon, Metall. Mater. Trans., A29, 1998, 2245.
[12] M. Furukawa, Z. Horita, M. Nemoto, R.Z. Valiev, T.G. Langdon, Acta Mater., 44, 1996, 4619.
[13] M. Furukawa, Z. Horita, T.G. Langdon, Mater. Sci. Eng., A332, 2002, 97.
[14] Y.T. Zhu, T.C. Lowe, Mater. Sci. Eng., A291, 2000, 46.
[15] J.A. Wert, Q. Liu, N. Hansen, Acta Mater., 45, 1997, 2565.
[16] D.A. Hughes, Mater. Sci. Eng., A319-321, 2001, 46.
[17] Q. Liu, X. Huang, D.J. Lloyd, N. Hansen, Acta Mater., 50, 2002, 3789.
[18] P.J. Hurley, P.S. Bate, F.J. Humphreys, Acta Mater., 51, 2003, 4737.
[19] H. Weiland, Acta Metall., 40, 1992, 1083.
[20] A. Godfrey, D.A. Hughes, Acta Mater., 48, 2000, 1897.
[21] Q. Liu, N. Hansen, Scripta Metall. Mater., 32, 1995, 1289.
[22] D. Kuhlmann-Wilsdorf, N. Hansen, Scripta Metall., 25, 1991, 1557.
[23] P.L. Sun, P.W. Kao, C.P. Chang, Scripta Mater., 51, 2004, 565.
[24] P.L. Sun, P.W. Kao, C.P. Chang, Metall. Mater. Trans., A35, 2004, 1359.
[25] N. Hansen, D. Juul Jensen, Acta Metall., 40, 1992, 3265.
[26] D. Kuhlmann-Wilsdorf, Mater. Sci. Eng., A113, 1989, 1.
[27] D.A. Hughes, N. Hansen, Acta Mater., 48, 2000, 2985.
[28] E. Nes, A.L. Dons, N. Ryum, Ed. R.C. Gifkins, ICSMA 6, Pergamon Press, 1982, 425.
[29] D.A. Hughes, N. Hansen, Acta Mater., 45, 1997, 3871.
[30] B. Bay, N. Hansen, D.A. Hughes, D. Kuhlmann-Wilsdorf, Acta Metall. Mater., 40, 1992, 205.
[31] M.F. Ashby, Phil. Mag., 21, 1970, 399.
[32] D.A. Hughes, M.E. Kassner, M.G. Stout, J. Vetrano, J. Metals, 50, 1998, 16.
[33] R.D. Doherty, D.A. Hughes, F.J. Humphreys, J.J. Jonas, D. Juul Jensen, M.E. Kassner, W.E. King, T.R. McNelley, H.J. McQueen, A.D. Rollett, Mater. Sci. Eng., A238, 1997, 274.
[34] S.D. Terhune, D.L. Swisher, K. Oh-Ishi, Z. Horita, T.G. Langdon, T.R. McNelley, Metall. Mater. Trans., A33, 2002, 2173.
[35] F.R.N. Nabarro, D. Kuhlmann-Wilsdorf, Scripta Mater., 35, 1996, 1331.
[36] R.Z. Valiev, A.V. Kornizov, R.R. Mulyukov, Mater. Sci. Eng. A168, 1993, 141.
[37] Q. Liu, H. Xiaooxu, Y. Mei, Ultramicroscopy, 41, 1992, 317.
[38] M. Cabibbo, E. Evangelista, V. Latini, J. Mater. Sci., 39, 2004, 5659.